Sussex Research Online

Effect of high pressure homogenization on physicochemical properties of curcumin nanoparticles prepared by antisolvent crystallization using HPMC or PVP

Article (Accepted Version)

Homayouni, Alireza, Sohrabi, Masoumeh, Amini, Marjan, Varshosaz, Jaleh and Nokhodchi, Ali (2018) Effect of high pressure homogenization on physicochemical properties of curcumin nanoparticles prepared by antisolvent crystallization using HPMC or PVP. Materials Science and Engineering: C. ISSN 09284931

This version is available from Sussex Research Online: http://sro.sussex.ac.uk/id/eprint/81065/

This document is made available in accordance with publisher policies and may differ from the published version or from the version of record. If you wish to cite this item you are advised to consult the publisher's version. Please see the URL above for details on accessing the published version.

Copyright and reuse:
Sussex Research Online is a digital repository of the research output of the University.

Copyright and all moral rights to the version of the paper presented here belong to the individual author(s) and/or other copyright owners. To the extent reasonable and practicable, the material made available in SRO has been checked for eligibility before being made available.

Copies of full text items generally can be reproduced, displayed or performed and given to third parties in any format or medium for personal research or study, educational, or not-for-profit purposes without prior permission or charge, provided that the authors, title and full bibliographic details are credited, a hyperlink and/or URL is given for the original metadata page and the content is not changed in any way.

http://sro.sussex.ac.uk

Accepted Manuscript

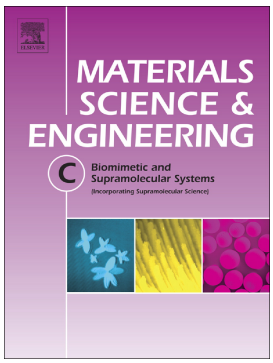

Effect of high pressure homogenization on physicochemical properties of curcumin nanoparticles prepared by antisolvent crystallization using HPMC or PVP

Alireza Homayouni, Masoumeh Sohrabi, Marjan Amini, Jaleh Varshosaz, Ali Nokhodchi

PII: S0928-4931(18)32685-7
DOI: https://doi.org/10.1016/j.msec.2018.12.128
Reference: MSC 9238

To appear in: *Materials Science & Engineering C*

Received date: 5 September 2018
Revised date: 11 December 2018
Accepted date: 28 December 2018

Please cite this article as: Alireza Homayouni, Masoumeh Sohrabi, Marjan Amini, Jaleh Varshosaz, Ali Nokhodchi , Effect of high pressure homogenization on physicochemical properties of curcumin nanoparticles prepared by antisolvent crystallization using HPMC or PVP. Msc (2018), https://doi.org/10.1016/j.msec.2018.12.128

This is a PDF file of an unedited manuscript that has been accepted for publication. As a service to our customers we are providing this early version of the manuscript. The manuscript will undergo copyediting, typesetting, and review of the resulting proof before it is published in its final form. Please note that during the production process errors may be discovered which could affect the content, and all legal disclaimers that apply to the journal pertain.

ACCEPTED MANUSCRIPT

Effect of high pressure homogenization on physicochemical properties of Curcumin nanoparticles prepared by antisolvent crystallization using HPMC or PVP

Alireza Homayouni[a,*], Masoumeh Sohrabi[a], Marjan Amini[a], Jaleh Varshosaz[a], Ali Nokhodchi[b,*]

[a]Department of Pharmaceutics, School of Pharmacy and Novel Drug Delivery Systems Research Center, Isfahan University of Medical Sciences, Isfahan, Iran,

[b]Pharmaceutics Research Laboratory, Arundel Building, School of Life Sciences, University of Sussex, Brighton, BN1 9QJ, UK

*Corresponding authors: Alireza Homayouni (a.r.homayouni@gmail.com, a.r.homayouni@pharm.mui.ac.ir) and Ali Nokhodchi (a.nokhodchi@sussex.ac.uk)

ACCEPTED MANUSCRIPT

ACCEPTED MANUSCRIPT

Abstract

Dissolution enhancement of poorly water soluble drugs is a major challenge in pharmaceutical industry. The aim of this study is to fabricate curcumin nanoparticles by antisolvent crystallization in the presence of PVP-K30 or HPMC with various concentrations as a stabilizer. The effect of high pressure homogenization on properties of curcumin particles is also investigated in this study. The antisolvent crystallization method followed by freeze drying (CRS-FD) and also antisolvent crystallization and high pressure homogenization followed by freeze drying (HPH-FD) were employed to modify curcumin particles. Physical mixtures of the drug and additives were also prepared for comparison purposes. The solid state analysis (DSC, XRPD and FT-IR studies), particle size measurement, morphological analysis, saturation solubility and dissolution behavior of the samples were investigated. The curcumin crystallized without using stabilizer produced polymorph 2 curcumin with lower crystallinity and higher solubility. The samples obtained in the presence of stabilizers showed higher solubility compared to its physical mixtures counterpart. It was found that the stabilizers used in the current study were capable of inhibiting the crystal growth of particles during crystallization. High pressure homogenizer method generated smaller particles compared to those samples that were not subjected to high pressure homogenizer (for example, 2748 nm for 5% PVP CRS-FD sample and 706 nm for 5% PVP HPH-FD sample). Particles obtained via HPH showed better solubility and dissolution rate compared to those samples that HPH was not employed (for example, the saturated solubility of 25% PVP CRS-FD sample was near 2 µg/ml while this amount was approximately 4.3 µg/ml for 25% HPH-FD sample. The effect of high pressure homogenization on dissolution rate is more pronounced for samples with lower stabilizer ratio. The samples prepared with high pressure homogenizer using 50% PVP showed 25-fold higher solubility compared to untreated curcumin. Generally, it can be concluded that the method of preparation, selection of suitable stabilizer and concentration of stabilizer play a critical role on particle size and dissolution rate of curcumin.

Keywords: curcumin, antisolvent crystallization, dissolution rate, high pressure homogenization

ACCEPTED MANUSCRIPT

1. Introduction

Formulation of poorly water soluble drugs is a major challenge in the pharmaceutical industry. There are many strategies which have been used before for improving the solubility and dissolution rate of poorly water soluble drugs [1]. Reduction of particle size to nanoscale is the most favorable way which has been used in last decades. According to Noyes-Whitney equation, reducing the particle size results in higher surface area and hence higher dissolution rate. Beside that reduction in the particle size to the nanometer size increases the saturation solubility due to the Ostwald-Freundlich equation which is normally not obtained when the particles are micronized [2, 3].

In general, preparation of nanoparticles can be reached by two strategies; bottom up and top down methods [2]. In the pharmaceutical industry nanoparticles are mainly produced by top down strategy [4]. High pressure homogenization (HPH) and media milling are the most favorable methods to produce these nanoscale materials [3, 5]. In these methods the particles break down to nanoscale size by attrition, collision and sometimes cavitation especially for HPH process. However, these methods suffer from some disadvantages. In most of the time, the preparation of nanoparticles with these methods need high energy input, long time processing, wide particle size distribution and probability of metal consumption [4, 6]. In contrast to top down procedure, in bottom up strategy nanoparticles can be obtained by molecular arrangements. One of the simplest and cost effective methods for preparation of nanoparticles via this strategy is antisolvent crystallization technique. In this method, simply the solubilized drug in an organic solvent is added to an antisolvent that is miscible with the first solvent. In most cases, water has been used as an antisolvent. The precipitated drug could be separated by filtration, spray drying or freeze drying techniques. This method does not need any expensive equipment, high energy input or long processing time. In addition, particle engineering and crystal manipulation could be performed by this method [7, 8]. In addition, supercritical fluid techniques have been used for producing small and nanosized particles [9-11]. However, preventing the crystal growth is the biggest problem in this process. In order to tackle this problem, the addition of stabilizers could inhibit crystal growth of drugs by adsorbing to the surface of obtained crystals. Various stabilizers have been used for this purpose [12]. As in most cases these stabilizers are hydrophilic, therefore, the presence of these stabilizers could also be beneficial in order to improve the solubility properties of poorly

ACCEPTED MANUSCRIPT

water soluble APIs. However, it has been shown that different stabilizers do not exhibit the same effect on crystal growth of the crystals during the crystallization process [12].

Although the antisolvent crystallization could engineer the nanoparticles by molecular arrangement, however, as described before it suffered from crystal growth [7]. In last decade, a combination process has been used in many studies such as Nanoedge® technology (used by Baxter Inc.) where precipitation was coupled with HPH. In this process antisolvent crystallization combined with high pressure homogenization during crystallization or after it. In this method the aggregated particles could be broken down to lower particle size. In addition, amorphous or unstable particles obtained during antisolvent crystallization could convert to more stable form after HPH process [5, 13]. This combination process has been used for different poorly water soluble drugs like itraconazole [14], isradipine [15] and celecoxib [16, 17].

Curcumin is a hydrophobic phenolic compound which is extracted from the rhizome of turmeric. This substance showed some various pharmacological activities such as anticancer, antioxidant, anti-inflammatory, and antimicrobial properties ,however, due to its poor water solubility (11 ng/ml at pH 5.0) its oral bioavailability is limited and incomplete [18]. Various attempts have been used in the past to overcome this problem. Reducing the particle size [19-21], preparation of solid dispersion [22, 23], solid lipid nanoparticles [24], nanomicelles [25, 26], and using cyclodextrins [27] are some examples which have been explored. The aim of this study was to prepare curcumin nanoparticles with a better dissolution behavior. Antisolvent crystallization in the presence of HPMC and PVP at various concentrations as a stabilizer has been used in this study. In addition, the effect of high pressure homogenization process was employed to optimize the physiochemical properties of curcumin particles.

2. Materials and methods

2.1. Materials

Curcumin was purchased from Mitushi Biopharma, India (pharmaceutical grade). PVP-K30 and HPMC E3 were purchased from Sigma-Aldrich, Germany (Pharmaceutical grade). Acetone and sodium dodecyl sulfate (SDS) were obtained from Merck (analytical grade).

ACCEPTED MANUSCRIPT

2.2. Methods

2.2.1. Preparation of CUR:HPMC and CUR:PVP freeze dried nanoparticles precipitated by antisolvent crystallization method (CRS-FD)

1 gram of curcumin was dissolve in 20 ml of acetone. Then the acetone solution containing curcumin was added to the 200 ml aqueous solution contain 0, 50, 100, 250 and 500 mg stabilizer (PVP or HPMC) at a rate of 5 ml/min using a burette. The aqueous solution was kept under stirring condition at 600 rpm and the temperature was kept at 25 °C during precipitation. The final concentration of each suspension was 1:0, 20:1, 10:1, 4:1 or 2:1 curcumin:polymer respectively. The final suspension was immediately freeze dried at -70 °C followed by freeze drying (Martin Christ freeze dryer, Germany) for 48 h. Each crystallization experiment was performed in triplicate.

2.2.2. Preparation of CUR:HPMC and CUR:PVP freeze dried nanoparticles precipitated by antisolvent crystallization method followed by high pressure homogenizer (HPH-FD)

Half part of the obtained suspenstions from previous method (CRS) were further homogenized with A FBF laboratory high pressure homogenizer (Italy). The applied pressure was set at 500 bars for 5 cycles (first step) and 1000 bars for 10 cycles (final step). The final suspension obtained after applying HPH was immediately freeze- dried at -70 °C for 48 h. Each experiment was performed at least three times.

2.2.3. Preparation of physical mixtures of drug carrier (PM)

Physical mixtures of CUR and stabilizer were prepared as the same ratios as the treated formulations r comparison purposes. To this end, CUR, HPMC or PVP were sieved to get particle size fractions of less than 250 µm followed by mixing of CUR with HPMC or PVP using a spatula for 2 min. The formulations were kept in well-tight containers until further use.

ACCEPTED MANUSCRIPT

2.2.4. Morphological analysis

Optical microscope (Olympus BX-60, Japan) was used to observe particles formation during the manufacturing process before freeze drying. In addition, SEM images of the freeze-dried particles were obtained using a scanning electron microscope (Philips X series, Netherlands) with an acceleration voltage of20 kV.

2.2.5. Particle size measurement

In order to measure the particle size of particles obtained via CRS and HPH process a nano-zetasizer (Malvern, UK) was used. To do this end, the obtained nanosuspension was diluted with deionized water to reach the concentration of 1mg/ml. In the case of freeze dried samples this concentration was prepared by dispersing the powders in deionized water using ultrasound water bath (2 minutes). The measurements were carried out in triplicate and their mean and standard deviation of Z-average size and zeta potential of the particles were calculated.

2.2.6. Saturation solubility study

Saturation solubility of untreated CUR, PMs and freeze dried samples obtained via different methods were determined according to the method published elsewhere [28]. An excess amount of CUR (2 mg) was dispersed in 20 ml double-distilled water in a beaker stirring at 200 rpm at 25 °C for 48 h. The suspensions were then filtered through a 0.22 µm filter (MS® Nylon Syringe Filter) and then the concentration of solution was measured by spectrophotometer at a wavelength of 426 nm (Shimadzu, Japan).

2.2.7. Differential scanning calorimetry (DSC)

Thermal analysis of selected freeze dried samples was carried out using DSC 822e (Mettler Toledo, Switzerland) equipped with a refrigerated cooling system. Few mg of the samples (2-3 mg) were placed in an aluminum pans and sealed with a lid. The samples were scanned from 20 to 200 °C at a rate of 10 °C/min. N_2 gas was used as an inert atmosphere at a flow rate of 80 ml/min. The thermal behaviors of the samples such as onset temperatures, endothermic and exothermic enthalpies were determined using the software provided (STARe Ver. 12.00 Mettler Toledo, Switzerland).

ACCEPTED MANUSCRIPT

In addition, the Gordon-Taylor equation (equation 1) has been used in order to estimate the theoretical T_{gmix} of samples and compare this value to experimental T_{gmix} of two components [29].

$$T_{gmix} = \frac{w_1 T_{g1} + k w_2 T_{g2}}{w_1 + k w_2} \qquad K \approx \frac{T_{g1}\rho_1}{T_{g2}\rho_2} \qquad \text{Equation 1}$$

In this equation w_1 and w_2 are the weight fraction of components 1 and 2. T_{g1} and T_{g2} is the glass transition of two components. ρ is the true density calculated by helium micrometers. The true density of amorphous CUR and PVP were determined 1.3 and 1.18 g/cm^3 respectively.

2.2.8. X-ray powder diffraction studies (XRPD)

The solid state of the freeze-dried samples was analyzed using XRPD. Scanning were carried out on selected samples using a D8 Advance diffractometer (Bruker, Germany) with Cu Kα radiation (λ = 1.54 Å) with scanning range of 5-40° (2Θ) with a step size of 0.05.

2.2.9. Fourier transform infrared spectroscopy (FT-IR)

FT-IR spectra were obtained with WQF-510/520 FT-IR spectrophotometer, China. Samples were prepared by mixing with potassium bromide (KBr) at a ratio of 1:10 and then compressed with hydraulic press at a pressure of 7 tones. The samples were scanned against a blank KBr disk ranging from 4000 to 450 cm^{-1} with a resolution of 1.0 cm^{-1}.

2.2.10. Dissolution studies

The dissolution properties of curcumin samples were examined using a USP dissolution apparatus 2, paddle method (Pharmatest, Germany). The dissolution medium was 1000 ml distilled water containing 0.25%w/v sodium dodecyl sulfate at 37 °C with the paddles rotation of 50 rpm. Samples equivalent to 10 mg of CUR was placed at the top of the dissolution medium. 5 ml of the dissolution medium was removed at selected time intervals and replaced by 5 ml fresh dissolution medium. Each sample was immediately filtered through 0.22 µm cellulose ester filter (MS® Nylon Syringe Filter) and assayed at a wavelength of 426 nm by spectrophotometer (Shimadzu, Japan).

ACCEPTED MANUSCRIPT

The concentration of the solution was then calculated on the basis of a calibration curve obtained for CUR at this wavelength. The dissolution test was repeated 3 times for each formulation.

The dissolution efficiency (DE%) and mean dissolution time (MDT) were determined in order to have a better understanding and comparison of dissolution profiles [30]. In equation 2, DE% represents the area under the dissolution curve (y) up to a certain time t, expressed as a percentage of the area of the rectangle described by 100% dissolution in the same time.

$$DE\% = \frac{\int_0^t y.dt}{y_{100}.t} \times 100 \qquad \text{Equation 2}$$

Equation 3 represents MDT and it reflects the mean time of dissolution. In equation 3 $\bar{t}_i$ defines the midpoint of the time period during which the fraction ΔM of the drug has been released from sample.

$$MDT = \sum \bar{t}_i .\Delta M_i / \sum \Delta M_i \qquad \bar{t}_i = (t_i + t_{i+1}) / 2 \qquad \Delta M_i = \left(M_{i+1} - M_i\right)$$

Equation 3

2.2.12. Re-dispersibility in water

In this test simply an excess amount of each freeze-dried samples were put on the surface of distilled water in a beaker and then re-dispersion of particles was recorded photographically after 3 seconds.

Although the dissolution studies provide suitable results and indirectly show how fast the particles could be dispersed and being wet in water, this test has been carried out to illustrate visually and supports the dissolution results.

3. Results and discussions

In this study antisolvent crystallization method was used in order to produce nanoparticles of curcumin with high water solubility. In addition, the effect of HPH process on solubility and

ACCEPTED MANUSCRIPT

dissolution rate of CUR was studied. It has been shown that the combination technology could result in smaller particles with narrow size distribution [13, 15, 16]. Moreover, in this study the efficiency of PVP-K30 and HPMC E3 as a stabilizer (at various ratios) has been evaluated.

3.1. Morphological analysis

The optical microscope screening was used in order to monitor the obtained suspensions. For better visualization of freeze-dried samples, scanning electron microscopy has been used.

Figure 1 shows the optical microscope images of freshly obtained suspensions. The freshly crystalized CUR obtained in the absence of any stabilizer showed aggregated particles with wide particle size distribution at a magnification of ×100 (Fig 1A). According to the hydrophobicity of CUR it could be predicted that the generated crystals could aggregate together and the crystals become large. This result has also been reported for CUR prepared with antisolvent crystallization [31, 32]. Yadav and Kumar reported that curcumin nanocrystals could be prepared by antisolvent precipitation however these particles aggregated simply after a while in the absence of any stabilizer. These aggregations and then an increase in the particle size did not occur when gelatin was used as a stabilizer [32].

As shown in Figure 1B very small and homogenous particles obtained after crystallization in the presence of stabilizers. Both PVP and HPMC at various concentrations showed similar morphology (for sake of space only one sample was shown). As described in the introduction section in order to produce nanoparticles with smaller particles size HPH was used. Interestingly, the samples introduced to HPH, produced suspensions with larger particle size and different shapes compared to CRS samples (Figure 1C). These samples showed platy-shape crystals instead of spherical particles obtained via CRS method. The formation of spherical particle (Figure 1B) could be due to the creation of temporary nanoemulsion droplets *(quasi-emulsion)* during the crystallization that has been reported before for celecoxib in our previous study [17]. When temporary nanoemulsions were formed, their structures could be destroyed by a high energy input such as HPH process and this in turn can lead to the formation of suspensions with different particle morphologies with a wider particle size distribution. Similar results have been reported when

ACCEPTED MANUSCRIPT

antisolvent precipitation technique was used to obtain celecoxib particles in the presence of d PVP-K30 [17].

The rupture of nanoemulsion droplets could be occurred by freeze drying process. Freeze-dried samples are shown in Figure 2. Untreated CUR shows irregular and large particles (Figure 2A) while the crystallized sample without usage of a stabilizer (CUR-CRS-FD) showed star-like large crystals. It seems during the crystallization process small crystals of CUR (because of its hydrophobic nature) aggregated together and become bigger after a while (Figure 2B). The star-like morphology of CUR prepared with antisolvent crystallization has also been reported and discussed elsewhere[31]. Generally, the crystalized samples showed platy-shape particles with smaller particle size. Figures 2C and 2D show the freeze dried samples crystallized in the present of 5% PVP without and with the employment of HPH process respectively. Both these samples exhibited platy-shape crystals and it seems HPH process could not affect the morphology of these samples, but as shown in this Figure the particle size of HPH-FD samples (Figure 2D) is smaller compared to when HPH was not used. In CUR:HPMC 5% CRS-FD sample some rode-shape crystals can be seen which these particles can be broken down to smaller particles and converted to platy-shape crystals with smaller particle size (Figure 2F).

Generally, it seems in freeze-dried samples, HPH process could break down the particles to smaller nanoscale particles with platy-shape crystal habit. This morphology could be useful in order to improve the dissolution rate due to high surface area available for dissolution.

3.2. Particle size measurement

Particle size analyses has been performed in order to investigate the effect of stabilizers with various concentrations and also the effect of HPH and freeze drying processes on particle size and Polydispersity Index (PdI) of the samples.

As shown in Table 1, the presence of stabilizers at various concentrations generated suspension with nanoscale particles. This occurrence demonstrated the beneficial effect of the presence of HPMC or PVP-K30 as stabilizer during the crystallization process. There is no significant different between the particle size of suspensions obtained with HPMC or PVP ($p > 0.05$). In addition, there

ACCEPTED MANUSCRIPT

is no significant different between the particle size at various concentrations of the stabilizers ($p > 0.05$).

The results in Table 1 showed that, in general, mean particle size and PdI of CRS samples are smaller than formulations obtained via HPH ($p < 0.05$). As described in the morphology section, the nanoemulsion obtained via CRS method could be broken down by HPH process and produce the suspensions with larger particle size.

The mean particle size of all freeze-dried samples are larger than non-freeze-dried samples. It is obvious that during freeze drying process the nanoparticles could aggregate together hence re-dispersion of these particles does not happen easily. It has been reported that the major challenge in formulation of pharmaceutical nanoparticles is their instability and aggregation of these nano-ranged particles. This phenomenon could be more problematic when the particles separated from a suspension and compress into a tablet [33, 34]. Regarding the zeta potential (Table 1) it seems that the samples obtained using PVP can be more stable than CUR:HPMC samples. It has been proved that in order to make a nanosuspension more stable a minimum zeta potential of ±30 mV is required. [35].

It was interesting to note that CRS samples showed smaller particles size compared to the samples obtained via HPH while the HPH-FD samples showed smaller particle size compared to CRS-FD samples. Generally, in these samples (HPH-FD) all the samples showed smaller particle size with lower PdI compared to similar CRS-FD samples. This phenomenon could be attributed to the ability of HPH process in order to separate the particles after being freeze- dried. Several studies reported that high pressure homogenizer could produce nanocrystals with narrow PdI with a suitable re-dispersibility [5].

3.3. Determination of saturation solubility

This analysis was performed in order to investigate the effect of hydrophilic stabilizers and methods of preparation on saturation solubility of CUR. The saturation solubility shows that untreated CUR exhibited very low saturation solubility (0.18 µg/ml) while the presence of hydrophilic stabilizer could enhance the solubility of CUR significantly ($p < 0.05$). This enhancement becomes more pronounced by the presence of higher stabilizer concentration.

ACCEPTED MANUSCRIPT

Comparing all the CRS-FD samples of HPMC and PVP with their physical mixtures (PMs) exhibited no significant difference between them, however, in general the PVP showed beneficial effect in order to increase the saturation solubility of CUR. This result was exhibited for both CRS-FD and PMs samples (Figure 3A and 3B). Figure 3 also showed that HPH-FD samples exhibited higher saturation solubility compared to CRS-FD and PMs samples and this enhancement is higher for PVP samples compared to HPMC samples. Statistical analysis demonstrated that saturation solubility of all CUR: PVP HPH-FD samples was higher compared to CRS-FD and PMs samples ($p < 0.05$). This was not the case for CUR:HPMC HPH-FD samples ($p > 0.05$). In general, it can be concluded that antisolvent crystallization technique followed by HPH could increase the saturation solubility of CUR with assistance of a stabilizer. In addition, it seems PVP-K30 shows a suitable efficiency compared to HPMC in terms of increasing the saturated solubility. It has been reported that the selection of an efficient stabilizer for a specific API in antisolvent precipitation technique depends on the physicochemical properties of API and stabilizer and there is no guarantee a specific stabilizer should work for all APIs with different physicochemical properties [12].

3.4. Differential scanning calorimetry (DSC)

Thermal analysis usually used to investigate the solid state of materials. Moreover, any interaction between API and stabilizer could be determined by this analysis. Figure 4 shows the DSC traces of untreated CUR and some selected samples. As shown in Figure 4, untreated CUR shows an endothermic peak near 176 °C corresponding to its melting point which reported in literature [36, 37]. The crystallized CUR without any stabilizer (CUR-CRS) showed two endothermic peaks near 162 °C and 157 °C. Comparison of these two thermograms demonstrated the presence of a new polymorph of CUR in CUR-CRS samples. In addition, the enthalpy of fusion in 2nd peak of CUR-CRS sample reduced from 82 J/g for untreated CUR to 74 J/g for newly prepared sample. This may be due to a slight reduction in the crystallinity of the sample which also has been reported elsewhere for curcumin when antisolvent crystallization was applied [31, 36, 38].

PM samples showed a broad melting endothermic peak near melting point of CUR. In these samples tailing the peaks to the left and expanding the peaks may be attributed to partial dissolution of CUR in stabilizers when it was heated above the T_g of polymers during DSC analysis. This

ACCEPTED MANUSCRIPT

result indicates the possibility of stabilizer/CUR miscibility. Similar results have been reported before for many API and polymers [39, 40]. CUR:HPMC 50% CRS-FD sample showed similar pattern to its PM sample. It seems in this sample there is no specific interaction between CUR and HPMC. The absence of CUR melting endothermic peak in CUR:PVP 50% CRS-FD formulation could be an indication of amorphous CUR in this sample. As shown in Figure 4 CUR:PVP 50% CRS-FD sample shows small endothermic peak near 148 °C attributed to T_{gmix} of binary mixture of CUR/PVP (this peak is not visible in small scale). According to Gordon-Taylor equation, ideal molecular mixing of two component resulted one T_{gmix} between the T_g of two components [29, 41]. The theoretical T_{gmix} of this binary mixture was calculated 85.5 °C (via equation 1) while the experimentally determined T_g of binary mixture obtained near 148 °C (Figure 4). This value is higher than the predicted T_{gmix} and indicates a strong interaction between CUR and PVP and confirms the rigidity of molecules in this sample. This positive deviation to higher temperature could be due to the intermolecular interaction or possibility of hydrogen bonding between CUR and PVP that will discuss in FT-IR study later.

3.5. X-ray powder diffraction studies (XRPD)

The results of XRPD analysis have been depicted in Figure 5. Untreated CUR showed sharp peaks at 2Θ values of 9.15°, 10.3°, 14.2°, 16.9°, 20.1° and 21.1° which regarded to its crystalline state [36]. CUR-CRS samples showed similar characteristic peaks but with lower peak intensity. This result demonstrates lower crystallinity of this sample compared to untreated one. In addition, in CUR-CRS sample the presence of a new peak at 16.2° 2Θ value indicated the appearance of a new polymorph in this sample. These results support the DSC findings and are in agreement with previous data [31, 38]. Sanuphi et al proved that the polymorph 2 exhibited lower crystallinity compared to polymorph 1 of curcumin [36]. Comparison of XRPD pattern of CUR-CRS to CUR-HPH exhibited that there is no different between these two samples. It seems HPH process does not modify the solid state of CUR during the homogenization process. Both crystalized samples containing 5% PVP exhibited similar pattern to the crystallized CUR however a small reduction in peak intensities are observed. For example, the intensity of peak at 16.2° 2Θ value is reduced. By increasing the polymer ratio to curcumin (in this case PVP) the peaks of CUR completely diminished, and hallo pattern is exhibited. This result indicated that CUR existed in amorphous

ACCEPTED MANUSCRIPT

state in this sample. It seems presence of high ratio of PVP as stabilizer could penetrate into the crystalline structure of CUR and converted the crystalline nature of CUR to amorphous form. This result confirmed the DSC finding. As described in DSC study this sample (CUR:PVP 50% CRS-FD) showed no endothermic peak and instead it exhibited one single T_g as a result of miscibility of CUR and PVP (as CUR:PVP 50% CRS-FD and CUR:PVP 50% HPH-FD sample showed similar XRPD pattern, therefore, XRPD of one sample shown). As shown in Figure 5, in CUR:HPMC 50% HPH-FD sample the intensity of CUR peaks reduced however the peak at 16.2° 2Θ is still visible. As described in DSC analysis it seems in this sample CUR does not present in amorphous state although the crystallinity of CUR decreased due to the presence of 50% HPMC as a polymer. Previous studies have been shown that the presence of polymer as a stabilizer during crystallization can reduce the crystallinity of drugs. This occurrence is due to the covering of particles by stabilizer during crystal growth phase of antisolvent precipitation process [16, 17, 21].

3.6. Fourier transform infrared spectroscopy (FT-IR)

FT-IR study was performed in order to investigate the possibility of hydrogen bonding between CUR and stabilizers during antisolvent crystallization. The FT-IR spectrums of untreated curcumin, CUR-CRS and crystalized samples prepared with 50% stabilizer were showed in Figure 6. As reported previous by other researchers, untreated curcumin (form 1) showed characteristic peaks at 1601 cm^{-1} belonged to aromatic C=C stretching, at 1429 cm^{-1} due to phenolic C-O stretching, at 1281 cm^{-1} due to enolic C-O stretching and a sharp peak at 3505 cm^{-1} which is attributed to OH stretching. In addition, as described in literature polymorph 1 curcumin shows a characteristic peak at 1628 cm^{-1} corresponded to its carbonyl group [36, 42]. Regularly carbonyl stretching band appear at 1700 cm^{-1} however formation of an intramolecular hydrogen bond leads to change of wave number to 1628 cm^{-1}. Resonance-assisted intramolecular hydrogen bond stabilized this conformation. It has been reported that this keto-enol tautomerism is the most favorable form of curcumin [36, 42].

CUR-CRS sample showed the same band at 1628 cm^{-1} indicating that the intramolecular hydrogen bonding keto-enol tautomer existed in this sample too. However, the OH stretching bond has been shifted to 3406 cm^{-1} and 3259 cm^{-1}. Moreover, the C=C aromatic stretching at 1601 cm^{-1} bifurcated to 1601 cm^{-1} and 1587 cm^{-1}. In addition, the phenolic C-O stretching at 1281 cm^{-1} bifurcated also

ACCEPTED MANUSCRIPT

to 1281 cm^{-1} and 1263 cm^{-1} (Figures 6A and 6B). All these changes demonstrated the formation of polymorph 2 CUR that Sanphui et al reported [36]. These findings are in good agreement with DSC and XRPD results.

As shown in Figure 6, PVP exhibited large and broad spectrum at 1668 cm^{-1} corresponding to C=O stretching vibration. It can be expecting that this group can participate in hydrogen bonding as a proton acceptor. In molecular structure of CUR, the possible proton donor could be the phenolic OH group. This possible hydrogen bonding should change the wave-number of these groups. The changes in OH groups position of CUR to 3406 cm^{-1} and broadening the peaks might be due to the presence of curcumin in amorphous nature [36]. Moreover, the presence of new wave-number at 3170 cm^{-1} could be attributed to the formation of hydrogen bond between CUR and PVP that previously reported by Wegiel et al in solid dispersion of CUR and PVP [42]. Due to the large number of carbonyl groups of PVP, the change in wave-number of this group is not simply visible. This phenomenon is attributed to the large number of unbounded carbonyl group of PVP compared to bounded group with OH group of CUR. FT-IR spectrum of CUR:HPMC 50% CRS-FD sample did not show any interaction between HPMC and CUR.

3.7. Dissolution studies

One of the main aims of the current research is dissolution enhancement of CUR. Therefore, dissolution studies were performed to investigate the effect of antisolvent crystallization method and HPH process on dissolution behavior of CUR. The dissolution behavior of untreated CUR and freeze-dried samples are shown in Figure 7. As shown in Figure 7, the untreated CUR shows very low dissolution rate even at 0.25% SDS. PMs of CUR with different concentrations of stabilizers are shown in Figures 7A and 7B. The dissolution rate of CUR increased by increasing the stabilizer ratio (Figure 7). PVP and HPMC as hydrophilic stabilizer could enhance the wettability of hydrophobic drugs and accelerate the dissolution rate of CUR. The dissolution properties of CRS-FD samples are shown in Figures 7C and 7D. In CUR:HPMC CRS-FD samples, the dissolution rate of CUR was not affected significantly. However, this was not the case for samples crystalized in the presence of PVP (Figure 7D). In these samples the dissolution rate of CUR increased compared to its PMs and this enhancement become more pronounced by increasing the PVP concentration. It can be concluded that antisolvent crystallization in the presence of PVP could

ACCEPTED MANUSCRIPT

produce particles with high dissolution rate. It seems the effect of PVP as a stabilizer plays a critical role on dissolution enhancement of CUR as the same enhancement in the dissolution rate was not observed for CUR-CRS-FD sample. On the other hand, the presence of PVP alone is not effective enough for dissolution enhancement of CUR as the dissolution rate of CUR did not increase sufficiently in its PM samples. In CUR:PVP CRS-FD samples an increase in the dissolution rate of curcumin become profound by increasing the PVP concentrations in the formulations. It seems the higher ratios of PVP could enhance the wettability of CUR hence facilitates the dissolution of curcumin. According to Figure 7D there is no remarkable difference between the dissolution rate of CUR:PVP 25% CRS-FD and CUR:PVP 50% CRS-FD samples. These samples showed DE of 82-83% and MDT of 6-7 min (Table 2). Figures 7E and 7F show the dissolution rate of HPH-FD samples. CUR-HPH-FD sample shows higher dissolution rate compared to untreated CUR and CUR-CRS-FD samples. Comparing the CUR:HPMC HPH-FD with CUR:HPMC CRS-FD samples shows that HPH technique could enhance the dissolution rate of CUR effectively. For instance, more than 80% of curcumin was released within 30 min from CUR:HPMC 25% HPH-FD sample while this value is lower than 30% for CUR:HPMC 25% CRS-FD sample. This enhancement in the percentage of dissolution of curcumin could be attributed to the presence of smaller particle size in these samples. According to the results of particle size analysis (Table 1) and SEM images (Figure 2), the HPH-FD samples exhibited smaller particle size and PdI compared to CRS-FD sample. For samples prepared with PVP as a stabilizer similar results were obtained. Comparing the Figures 7F and 7D show that HPH process enhanced the dissolution rate of almost all samples. This enhancement is more pronounced for samples prepared with lower PVP concentrations. According to Table 2 the amount of DE% and MDT for samples prepared with 25% and 50% PVP is almost similar to CRS-FD and HPH-FD formulations, while this similarity does not exist for the samples prepared with lower PVP concentration (5% and 10%). For example, in CUR:PVP 5% HPH-FD sample near 70% of CUR released after 10 min while this value is about 23% for CUR:PVP 5% CRS-FD sample. According to the results of particle size analysis and SEM images the HPH-FD samples exhibited smaller particle size and PdI compared to CRS-FD ones (similar to HPMC samples). Although the particle size is one of the most important parameters to control the dissolution rate and solubility of drugs however the effect of hydrophilic stabilizer (PVP in this case) should not be ignored. In other word, in the sample contain higher PVP percentage the effect of hydrophilic stabilizer controls the dissolution rate while in

ACCEPTED MANUSCRIPT

sample containing smaller ratio of PVP (5 and 10%) particle size plays a critical role on dissolution profile of CUR. In addition, according to DSC and XRPD studies sample prepared with 50% PVP contain amorphous CUR and simultaneously generated CUR/PVP matrix with a single T_g (Figure 4). Moreover, in this sample amorphous CUR participates in hydrogen bonding with PVP (Figure 6). All these findings justify the high dissolution rate and saturation solubility of CUR in crystalized samples contain 50% PVP. The higher solubility and dissolution rate of amorphous CUR compared to its crystalline form has been reported [36, 43]. Therefore, the effect of particle size is not determinative in samples crystallized in the presence of 50% PVP.

3.8. Re-dispersibility in water

This simple test has been performed to assess the dispersion of powders in water (as a first step of dissolution and finally absorption in the gastrointestinal tract) visually. In this test re-dispersion of samples recorded by digital camera after 3 second from placing a specified amount of powder on the surface of distilled water in a beaker. As shown in Figure 8A, untreated CUR does not disperse in water due to high hydrophobic nature, however in HPH-FD samples re-dispersion of particles occurred better. In samples prepared with 5% stabilizer (both PVP and HPMC) similar result was obtained. This phenomenon could be attributed to the presence of smaller particle size in HPH-FD samples. The results of this study are in good agreement with dissolution analysis. It has already been reported that nanoparticles prepared with high pressure homogenizer could re-disperse in water desirably [5].

4. Conclusion

It can be concluded that antisolvent crystallization followed by high pressure homogenization could be a useful procedure to prepare nanoparticles of curcumin with higher dissolution and saturation solubility. Using a suitable stabilizer plays a critical role on dissolution enhancement of curcumin during antisolvent crystallization. PVP as a stabilizer is able to inhibit the growth of particles during antisolvent crystallization technique. PVP can participate in hydrogen bonding with curcumin and reduces the crystallinity of curcumin. Formulation containing high concentration of PVP showed high dissolution rate even without using high pressure

ACCEPTED MANUSCRIPT

homogenization process. However, using high pressure homogenizer may help formulator prepare samples with low concentrations of PVP without compromising its dissolution rate. The results of this study showed that particle size, solid state of curcumin, presence of stabilizer, interaction of curcumin with stabilizers and in general physicochemical properties of samples play a critical role on dissolution rate of curcumin as well.

Acknowledgments

The authors thanked the Vice Chancellor Research of Isfahan University of Medical Sciences, Iran (Grant no. 294193) for the financial support.

References

[1] C.W. Pouton, Formulation of poorly water-soluble drugs for oral administration: Physicochemical and physiological issues and the lipid formulation classification system, European Journal of Pharmaceutical Sciences, 29 (2006) 278-287.
[2] R.H. Müller, S. Gohla, C.M. Keck, State of the art of nanocrystals – Special features, production, nanotoxicology aspects and intracellular delivery, European Journal of Pharmaceutics and Biopharmaceutics, 78 (2011) 1-9.
[3] E. Merisko-Liversidge, G.G. Liversidge, E.R. Cooper, Nanosizing: a formulation approach for poorly-water-soluble compounds, European Journal of Pharmaceutical Sciences, 18 (2003) 113-120.
[4] B. Van Eerdenbrugh, G. Van den Mooter, P. Augustijns, Top-down production of drug nanocrystals: Nanosuspension stabilization, miniaturization and transformation into solid products, International Journal of Pharmaceutics, 364 (2008) 64-75.
[5] C.M. Keck, R.H. Muller, Drug nanocrystals of poorly soluble drugs produced by high pressure homogenisation, European journal of pharmaceutics and biopharmaceutics : official journal of Arbeitsgemeinschaft fur Pharmazeutische Verfahrenstechnik e.V, 62 (2006) 3-16.
[6] F. Kesisoglou, S. Panmai, Y. Wu, Nanosizing — Oral formulation development and biopharmaceutical evaluation, Advanced Drug Delivery Reviews, 59 (2007) 631-644.
[7] B. Sinha, R.H. Müller, J.P. Möschwitzer, Bottom-up approaches for preparing drug nanocrystals: Formulations and factors affecting particle size, International Journal of Pharmaceutics, 453 (2013) 126-141.
[8] A. Nokhodchi, A. Homayouni, R. Araya, W. Kaialy, W. Obeidat, K. Asare-Addo, Crystal engineering of ibuprofen using starch derivatives in crystallization medium to produce promising ibuprofen with improved pharmaceutical performance, RSC Advances, 5 (2015) 46119-46131.

ACCEPTED MANUSCRIPT

[9] S.M. Abuzar, S.-M. Hyun, J.-H. Kim, H.J. Park, M.-S. Kim, J.-S. Park, S.-J. Hwang, Enhancing the solubility and bioavailability of poorly water-soluble drugs using supercritical antisolvent (SAS) process, International Journal of Pharmaceutics, 538 (2018) 1-13.
[10] V. Prosapio, E. Reverchon, I. De Marco, Formation of PVP/nimesulide microspheres by supercritical antisolvent coprecipitation, The Journal of Supercritical Fluids, 118 (2016) 19-26.
[11] I. García-Casas, A. Montes, C. Pereyra, E.J. Martínez de la Ossa, Co-precipitation of mangiferin with cellulose acetate phthalate by Supercritical antisolvent process, Journal of CO2 Utilization, 22 (2017) 197-207.
[12] A.A. Thorat, S.V. Dalvi, Liquid antisolvent precipitation and stabilization of nanoparticles of poorly water soluble drugs in aqueous suspensions: Recent developments and future perspective, Chemical Engineering Journal, 181–182 (2012) 1-34.
[13] B.E. Rabinow, Nanosuspensions in drug delivery, Nature reviews. Drug discovery, 3 (2004) 785-796.
[14] M. Chaubal, C. Popescu, Conversion of Nanosuspensions into Dry Powders by Spray Drying: A Case Study, Pharmaceutical research, 25 (2008) 2302-2308.
[15] D.B. Shelar, S.K. Pawar, P.R. Vavia, Fabrication of isradipine nanosuspension by anti-solvent microprecipitation–high-pressure homogenization method for enhancing dissolution rate and oral bioavailability, Drug Delivery and Translational Research, 3 (2013) 384-391.
[16] A. Homayouni, F. Sadeghi, J. Varshosaz, H. Afrasiabi Garekani, A. Nokhodchi, Promising dissolution enhancement effect of soluplus on crystallized celecoxib obtained through antisolvent precipitation and high pressure homogenization techniques, Colloids and Surfaces B: Biointerfaces, 122 (2014) 591-600.
[17] A. Homayouni, F. Sadeghi, J. Varshosaz, H.A. Garekani, A. Nokhodchi, Comparing various techniques to produce micro/nanoparticles for enhancing the dissolution of celecoxib containing PVP, European Journal of Pharmaceutics and Biopharmaceutics, 88 (2014) 261-274.
[18] A. Goel, A.B. Kunnumakkara, B.B. Aggarwal, Curcumin as "Curecumin": From kitchen to clinic, Biochemical Pharmacology, 75 (2008) 787-809.
[19] A. Beloqui, R. Coco, P.B. Memvanga, B. Ucakar, A. des Rieux, V. Préat, pH-sensitive nanoparticles for colonic delivery of curcumin in inflammatory bowel disease, International Journal of Pharmaceutics, 473 (2014) 203-212.
[20] M.M. Fares, M.t.S. Salem, Dissolution enhancement of curcumin via curcumin–prebiotic inulin nanoparticles, Drug Development and Industrial Pharmacy, 41 (2015) 1785-1792.
[21] F. Sadeghi, M. Ashofteh, A. Homayouni, M. Abbaspour, A. Nokhodchi, H.A. Garekani, Antisolvent precipitation technique: A very promising approach to crystallize curcumin in presence of polyvinyl pyrrolidon for solubility and dissolution enhancement, Colloids and Surfaces B: Biointerfaces, 147 (2016) 258-264.
[22] S.-W. Seo, H.-K. Han, M.-K. Chun, H.-K. Choi, Preparation and pharmacokinetic evaluation of curcumin solid dispersion using Solutol® HS15 as a carrier, International Journal of Pharmaceutics, 424 (2012) 18-25.
[23] J. Li, I.W. Lee, G.H. Shin, X. Chen, H.J. Park, Curcumin-Eudragit® E PO solid dispersion: A simple and potent method to solve the problems of curcumin, European Journal of Pharmaceutics and Biopharmaceutics, 94 (2015) 322-332.
[24] V. Kakkar, A.K. Mishra, K. Chuttani, I.P. Kaur, Proof of concept studies to confirm the delivery of curcumin loaded solid lipid nanoparticles (C-SLNs) to brain, International Journal of Pharmaceutics, 448 (2013) 354-359.

ACCEPTED MANUSCRIPT

[25] A.H. Abouzeid, N.R. Patel, V.P. Torchilin, Polyethylene glycol-phosphatidylethanolamine (PEG-PE)/vitamin E micelles for co-delivery of paclitaxel and curcumin to overcome multi-drug resistance in ovarian cancer, International Journal of Pharmaceutics, 464 (2014) 178-184.
[26] Z. Song, W. Zhu, N. Liu, F. Yang, R. Feng, Linolenic acid-modified PEG-PCL micelles for curcumin delivery, International Journal of Pharmaceutics, 471 (2014) 312-321.
[27] H.H. Tønnesen, M. Másson, T. Loftsson, Studies of curcumin and curcuminoids. XXVII. Cyclodextrin complexation: solubility, chemical and photochemical stability, International Journal of Pharmaceutics, 244 (2002) 127-135.
[28] R. Ghanavati, A. Taheri, A. Homayouni, Anomalous dissolution behavior of celecoxib in PVP/Isomalt solid dispersions prepared using spray drier, Materials Science and Engineering: C, 72 (2017) 501-511.
[29] J.A. Baird, L.S. Taylor, Evaluation of amorphous solid dispersion properties using thermal analysis techniques, Advanced Drug Delivery Reviews, 64 (2012) 396-421.
[30] F.O. Costa, J.J. Sousa, A.A. Pais, S.J. Formosinho, Comparison of dissolution profiles of Ibuprofen pellets, Journal of controlled release : official journal of the Controlled Release Society, 89 (2003) 199-212.
[31] A.A. Thorat, S.V. Dalvi, Particle formation pathways and polymorphism of curcumin induced by ultrasound and additives during liquid antisolvent precipitation, CrystEngComm, 16 (2014) 11102-11114.
[32] D. Yadav, N. Kumar, Nanonization of curcumin by antisolvent precipitation: process development, characterization, freeze drying and stability performance, Int J Pharm, 477 (2014) 564-577.
[33] J. Hu, K.P. Johnston, R.O. Williams, 3rd, Nanoparticle engineering processes for enhancing the dissolution rates of poorly water soluble drugs, Drug Dev Ind Pharm, 30 (2004) 233-245.
[34] E. Merisko-Liversidge, G.G. Liversidge, Nanosizing for oral and parenteral drug delivery: A perspective on formulating poorly-water soluble compounds using wet media milling technology, Adv Drug Deliv Rev, DOI (2011).
[35] R.H. Müller, C. Jacobs, O. Kayser, Nanosuspensions as particulate drug formulations in therapy: Rationale for development and what we can expect for the future, Advanced Drug Delivery Reviews, 47 (2001) 3-19.
[36] P. Sanphui, N.R. Goud, U.B. Khandavilli, S. Bhanoth, A. Nangia, New polymorphs of curcumin, Chem Commun (Camb), 47 (2011) 5013-5015.
[37] M. Kakran, N. Sahoo, I.L. Tan, L. Li, Preparation of nanoparticles of poorly water-soluble antioxidant curcumin by antisolvent precipitation methods, J Nanopart Res, 14 (2012) 1-11.
[38] A.A. Thorat, S.V. Dalvi, Solid-State Phase Transformations and Storage Stability of Curcumin Polymorphs, Crystal Growth & Design, 15 (2015) 1757-1770.
[39] A. Homayouni, F. Sadeghi, A. Nokhodchi, J. Varshosaz, H.A. Garekani, Preparation and characterization of celecoxib dispersions in soluplus®: Comparison of spray drying and conventional methods, Iranian Journal of Pharmaceutical Research, 14 (2015) 35-50.
[40] G. Terife, P. Wang, N. Faridi, C.G. Gogos, Hot melt mixing and foaming of soluplus® and indomethacin, Polymer Engineering and Science, 52 (2012) 1629-1639.
[41] A.F. Rumondor, I. Ivanisevic, S. Bates, D. Alonzo, L. Taylor, Evaluation of Drug-Polymer Miscibility in Amorphous Solid Dispersion Systems, Pharmaceutical research, 26 (2009) 2523-2534.

ACCEPTED MANUSCRIPT

[42] L.A. Wegiel, Y. Zhao, L.J. Mauer, K.J. Edgar, L.S. Taylor, Curcumin amorphous solid dispersions: the influence of intra and intermolecular bonding on physical stability, Pharmaceutical development and technology, 19 (2014) 976-986.
[43] Y.B. Pawar, G. Shete, D. Popat, A.K. Bansal, Phase behavior and oral bioavailability of amorphous Curcumin, European Journal of Pharmaceutical Sciences, 47 (2012) 56-64.

ACCEPTED MANUSCRIPT

ACCEPTED MANUSCRIPT

Fig 1. Optical microscope image of (A) curcumin obtained from anti solvent crystallization (CUR-CRS), (B) curcumin obtained from anti solvent crystallization at presence of 5% stabilizer, (C) curcumin obtained from anti solvent crystallization followed by high pressure homogenization at presence of 5% stabilizer.

Fig 2. SEM image of (A) untreated curcumin, (B) CRS-FD samples without stabilizer, (C) CRS-FD samples with 5% PVP, (D) HPH-FD samples with 5% PVP, (E) CRS-FD samples with 5% HPMC, (F) HPH-FD samples with 5% HPMC.

Fig 3. Saturation solubility of untreated curcumin, samples prepared with physical mixture (PM), freeze-dried samples prepared by antisolvent crystallization (CRS-FD) and freeze dried samples prepared by antisolvent crystallization followed by high pressure homogenization (HPH-FD).

Fig4. DSC traces of pure CUR, physical mixture (PM), freeze-dried samples prepared by antisolvent crystallization (CUR-CRS-FD) and freeze-dried samples prepared by antisolvent crystallization in the presence of 50% of PVP or HPMC.

Fig 5. XRPD pattern of untreated CUR, samples prepared by antisolvent crystallization (CRS-FD) and samples prepared by antisolvent crystallization followed by high pressure homogenization (HPH-FD) in the presence of stabilizer.

Fig 6. FT-IR spectra of untreated CUR, freeze-dried samples obtained through antisolvent crystallization techniques (CRS) in the presence of 50% PVP or HPMC.

Fig 7. Dissolution profiles for different samples: (A, B) physical mixtures of CUR and stabilizers, (C, D) freeze-dried samples prepared by antisolvent crystallization with carriers, (E, F) freeze-dried samples prepared by antisolvent crystallization followed by high pressure homogenization of CUR and stabilizers (HPH-FD). (n = 3, and error bars are standard deviation).

Fig 8. Re-dispersion of different samples in distilled water. (A) without stabilizers, (B) with 5% HPMC, (C) with 5% PVP.

ACCEPTED MANUSCRIPT

Table 1. Particle size of untreated CUR and CUR:HPMC/PVP samples prepared by different procedures. antisolvent crystallization (CRS), antisolvent crystallization followed by high pressure homogenization (HPH). Freeze dried antisolvent crystallization (CRS-FD), freeze dried antisolvent crystallization followed by high pressure homogenization (HPH-FD).

Sample	**size CRS**	**PdI**	**Zeta-potential**	**size HPH**	**PdI**	**size CRS FD**	**PdI**	**size HPH FD**	**PdI**
CUR	ND	ND	ND	ND	ND	ND	ND	ND	ND
PVP 5%	272 ± 40	0.172 ± 0.041	-29	790 ± 32	0.425 ± 0.016	2748 ± 1251	1	706 ± 452	0.562 ± 0.098
PVP 10%	186 ± 16	0.258 ± 0.053	-24	532 ± 37	0.377 ± 0.021	3018 ± 825	0.982 ± 0.271	1073 ± 349	0.405 ± 0.102
PVP 25%	231 ± 38	0.176 ± 0.044	-33	439 ± 64	0.463 ± 0.082	3447 ± 317	0.856 ± 0.198	1024 ± 441	0.595 ± 0.097
PVP 50%	259 ± 21	0.161 ± 0.037	-25	563 ± 91	0.193 ± 0.022	2193 ± 290	0.597 ± 0.102	915 ± 398	0.715 ± 0.136
HPMC 5%	222 ± 13	0.425 ± 0.041	-24	1631 ± 84	0.844 ± 0.092	3224 ± 834	1	2101 ± 1201	0.892 ± 0.201
HPMC 10%	201 ± 13	0.377 ± 0.052	-25	599 ± 37	0.353 ± 0.028	2663 ± 650	0.968 ± 0.195	1512 ± 825	0.687 ± 0.085
HPMC 25%	197 ± 11	0.463 ± 0.037	-18	594 ± 49	0.488 ± 0.017	4374 ± 321	1	1389 ± 768	0.725 ± 0.091
HPMC 50%	210 ± 14	0.193 ± 0.021	-13	1244 ± 91	0.456 ± 0.029	2266 ± 345	0.416 ± 0.189	1225 ± 504	0.521 ± 0.234

ACCEPTED MANUSCRIPT

ACCEPTED MANUSCRIPT

Table 2. Dissolution efficiency (DE) and mean dissolution time (MDT) of untreated CUR and CUR:HPMC/PVP samples prepared with physical mixture (PM), antisolvent crystallization (CRS) and crystallization followed by high pressure homogenization (HPH).

Samples	DE_{40} %	MDT (min)	Samples	DE_{40} %	MDT (min)
CUR	7.81	19.38	**CUR**	7.81	19.38
CUR CRS-FD	10.93	16.16	**CUR CRS-FD**	10.93	16.16
CUR HPH-FD	14.34	15.44	**CUR HPH-FD**	14.34	15.44
HPMC 5% PM	12.67	11.77	**PVP 5% PM**	11.33	17.92
HPMC 10% PM	16.87	8.55	**PVP 10% PM**	23.85	6.84
HPMC 25% PM	17.82	11.96	**PVP 25% PM**	13.91	8.81
HPMC 50% PM	22.10	10.85	**PVP 50% PM**	22.96	10.49
HPMC 5% CRS-FD	23.82	8.19	**PVP 5% CRS-FD**	30.48	13.60
HPMC 10% CRS-FD	23.72	9.16	**PVP 10% CRS-FD**	64.62	5.71
HPMC 25% CRS-FD	24.33	9.67	**PVP 25% CRS-FD**	81.91	6.99
HPMC 50% CRS-FD	27.23	8.57	**PVP 50% CRS-FD**	82.58	6.16
HPMC 5% HPH-FD	49.77	11.80	**PVP 5% HPH-FD**	71.98	8.92
HPMC 10% HPH-FD	54.06	11.28	**PVP 10% HPH-FD**	78.93	6.45
HPMC 25% HPH-FD	72.44	5.44	**PVP 25% HPH-FD**	78.26	7.38
HPMC 50% HPH-FD	72.24	6.42	**PVP 50% HPH-FD**	78.22	7.91

ACCEPTED MANUSCRIPT

Highlights

- Curcumin nanoparticles were prepared by antisolvent crystallization and high pressure homogenization.
- The curcumin crystallized in the absence of stabilizer showed different polymorphic form for curcumin.
- The Presence of stabilizer and using high pressure homogenization improved the solubility of curcumin.
- High concentration of PVP produced amorphous curcumin nanoparticles.
- The samples prepared with high pressure homogenizer using 50% PVP showed 25-fold higher solubility compared to untreated curcumin.

ACCEPTED MANUSCRIPT

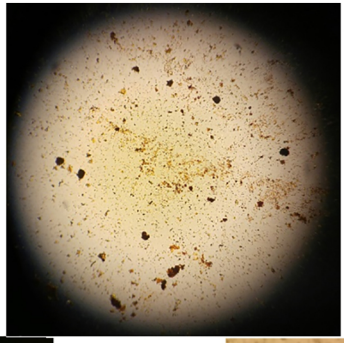

A

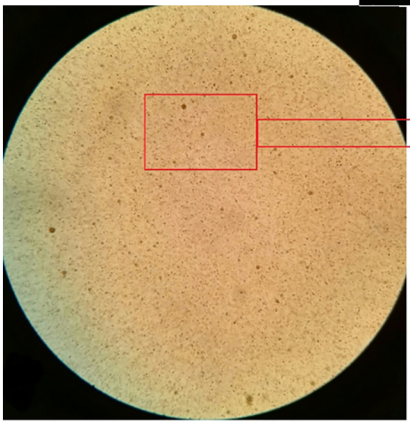

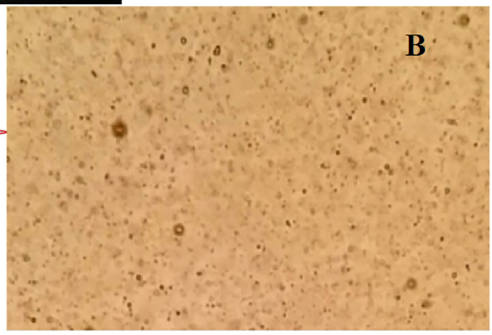

B

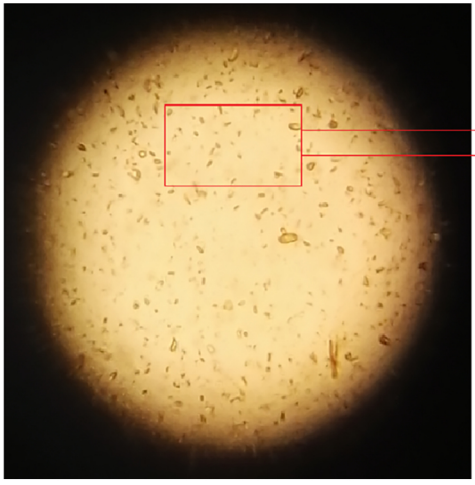

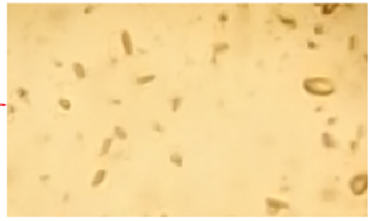

C

Figure 1

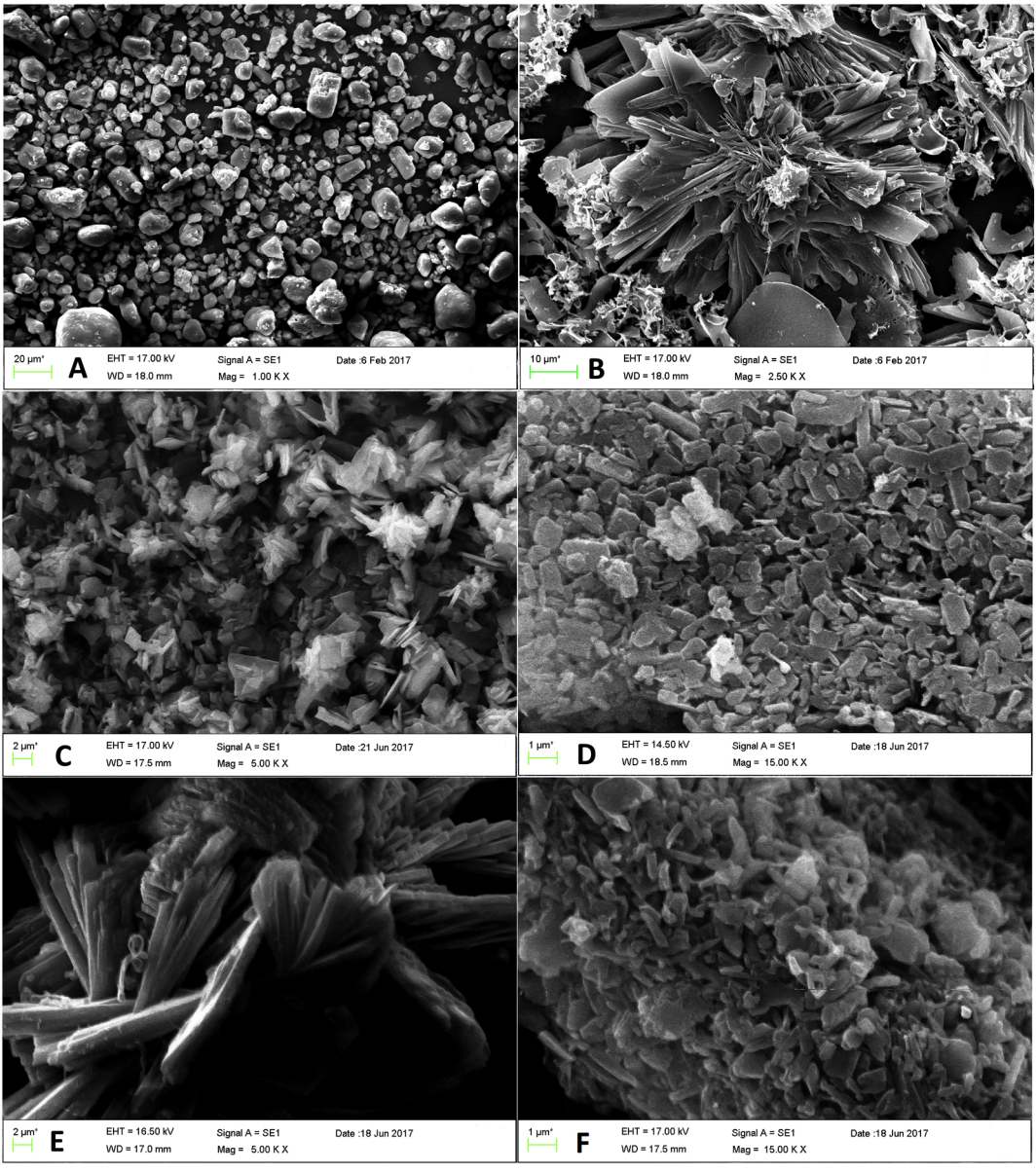
20 µm*
A
EHT = 17.00 kV
WD = 18.0 mm
Signal A = SE1
Mag = 1.00 K X
Date :6 Feb 2017
10 µm*
B
EHT = 17.00 kV
WD = 18.0 mm
Signal A = SE1
Mag = 2.50 K X
Date :6 Feb 2017
2 µm*
C
EHT = 17.00 kV
WD = 17.5 mm
Signal A = SE1
Mag = 5.00 K X
Date :21 Jun 2017
1 µm*
D
EHT = 14.50 kV
WD = 18.5 mm
Signal A = SE1
Mag = 15.00 K X
Date :18 Jun 2017
2 µm*
E
EHT = 16.50 kV
WD = 17.0 mm
Signal A = SE1
Mag = 5.00 K X
Date :18 Jun 2017
1 µm*
F
EHT = 17.00 kV
WD = 17.5 mm
Signal A = SE1
Mag = 15.00 K X
Date :18 Jun 2017

Figure 2

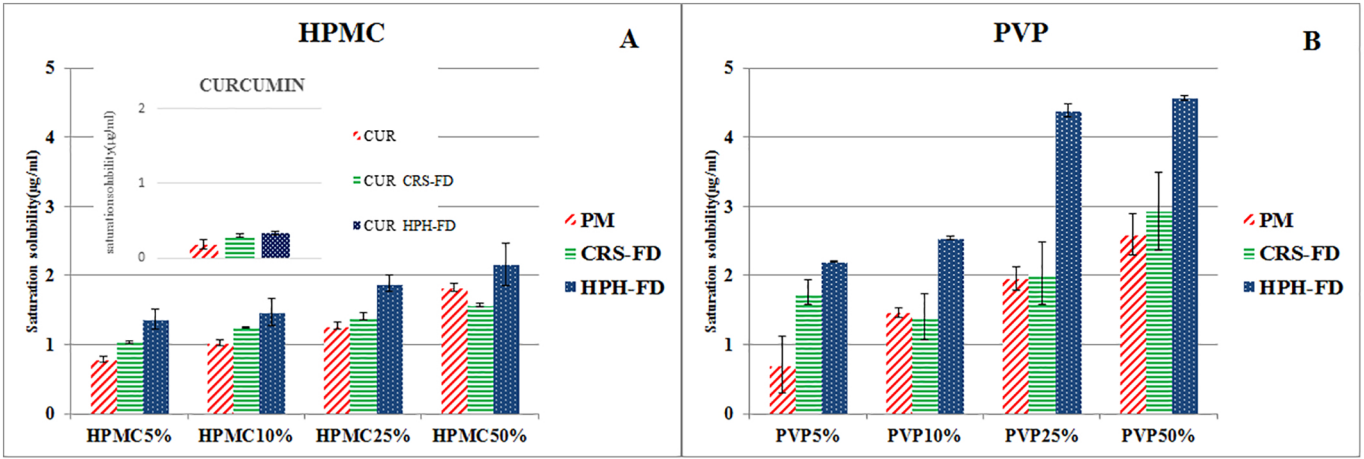
HPMC
A
CURCUMIN
saturationsolubility(µg/ml)
CUR
CUR CRS-FD
CUR HPH-FD
Saturation solubility(µg/ml)
PM
CRS-FD
HPH-FD
HPMC5%
HPMC10%
HPMC25%
HPMC50%
PVP
B
PVP5%
PVP10%
PVP25%
PVP50%

Figure 3

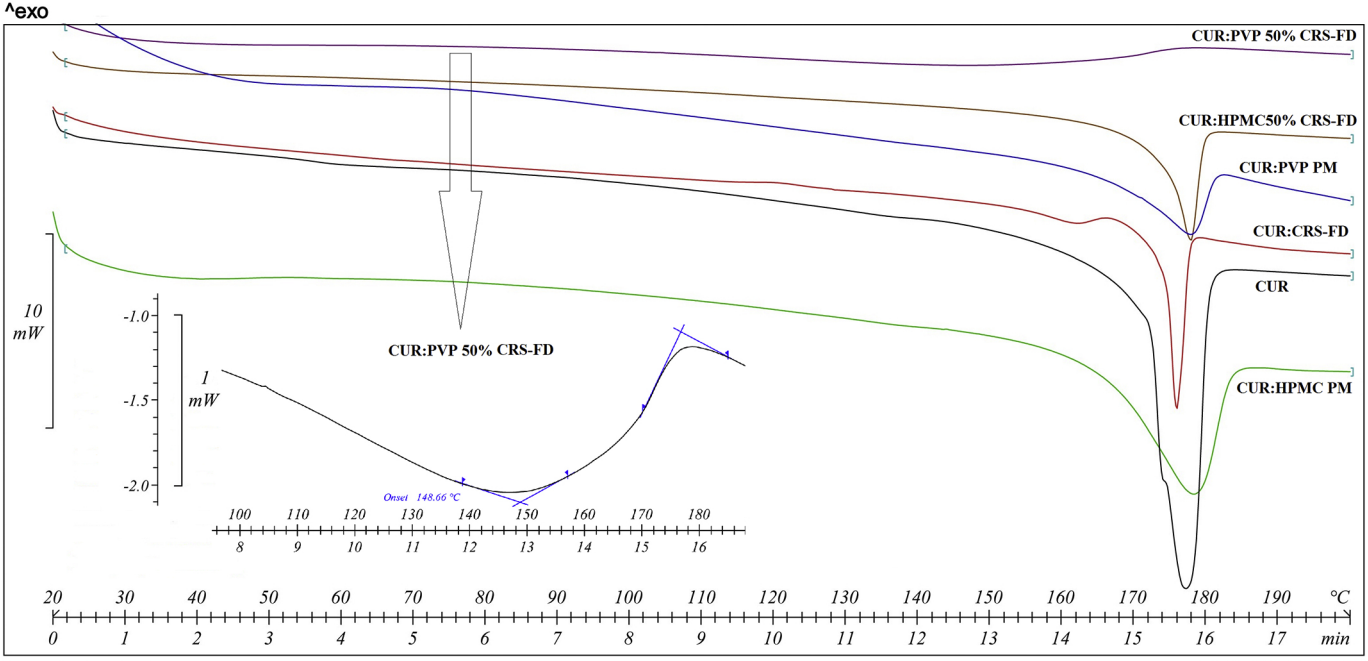
^exo
CUR:PVP 50% CRS-FD
CUR:HPMC50% CRS-FD
CUR:PVP PM
CUR:CRS-FD
CUR
CUR:HPMC PM
10 mW
-1.0
-1.5
-2.0
1 mW
CUR:PVP 50% CRS-FD
Onset 148.66 °C
100 110 120 130 140 150 160 170 180
8 9 10 11 12 13 14 15 16
20 30 40 50 60 70 80 90 100 110 120 130 140 150 160 170 180 190 °C
0 1 2 3 4 5 6 7 8 9 10 11 12 13 14 15 16 17 min
Lab: METTLER
STARe SW 12.00

Figure 4

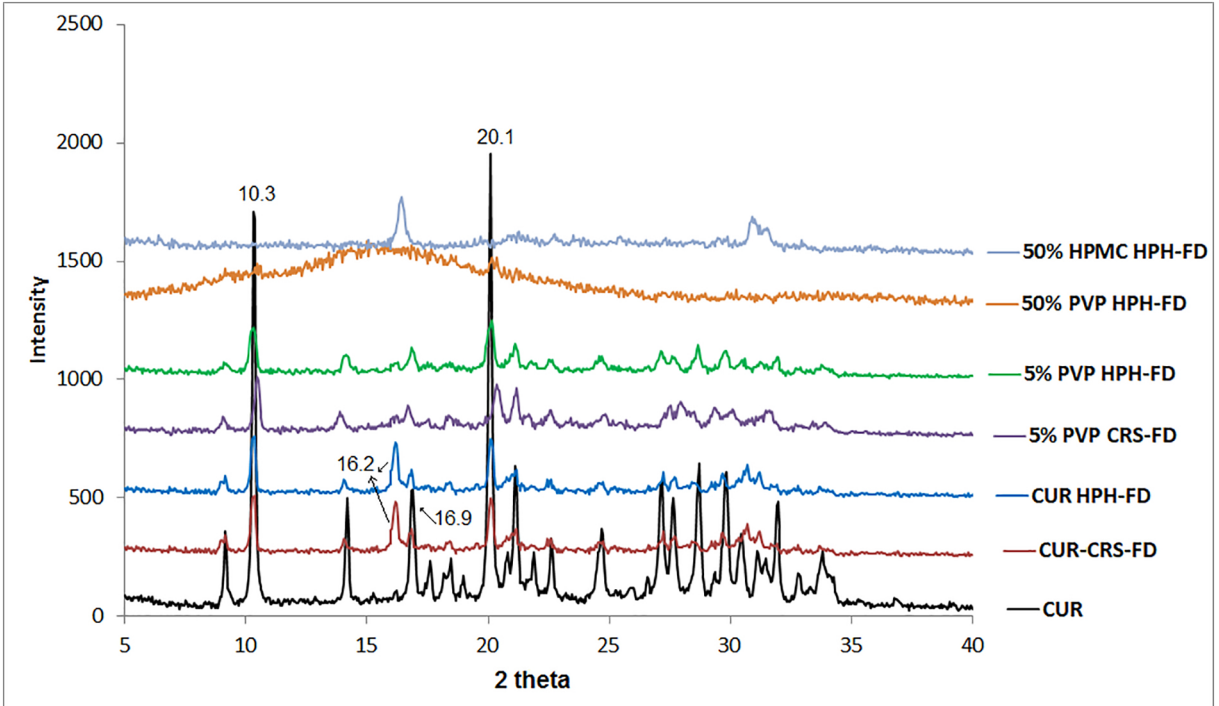
2500
2000
1500
1000
500
0
Intensity
5
10
15
20
25
30
35
40
2 theta
10.3
20.1
16.2
16.9
50% HPMC HPH-FD
50% PVP HPH-FD
5% PVP HPH-FD
5% PVP CRS-FD
CUR HPH-FD
CUR-CRS-FD
CUR

Figure 5

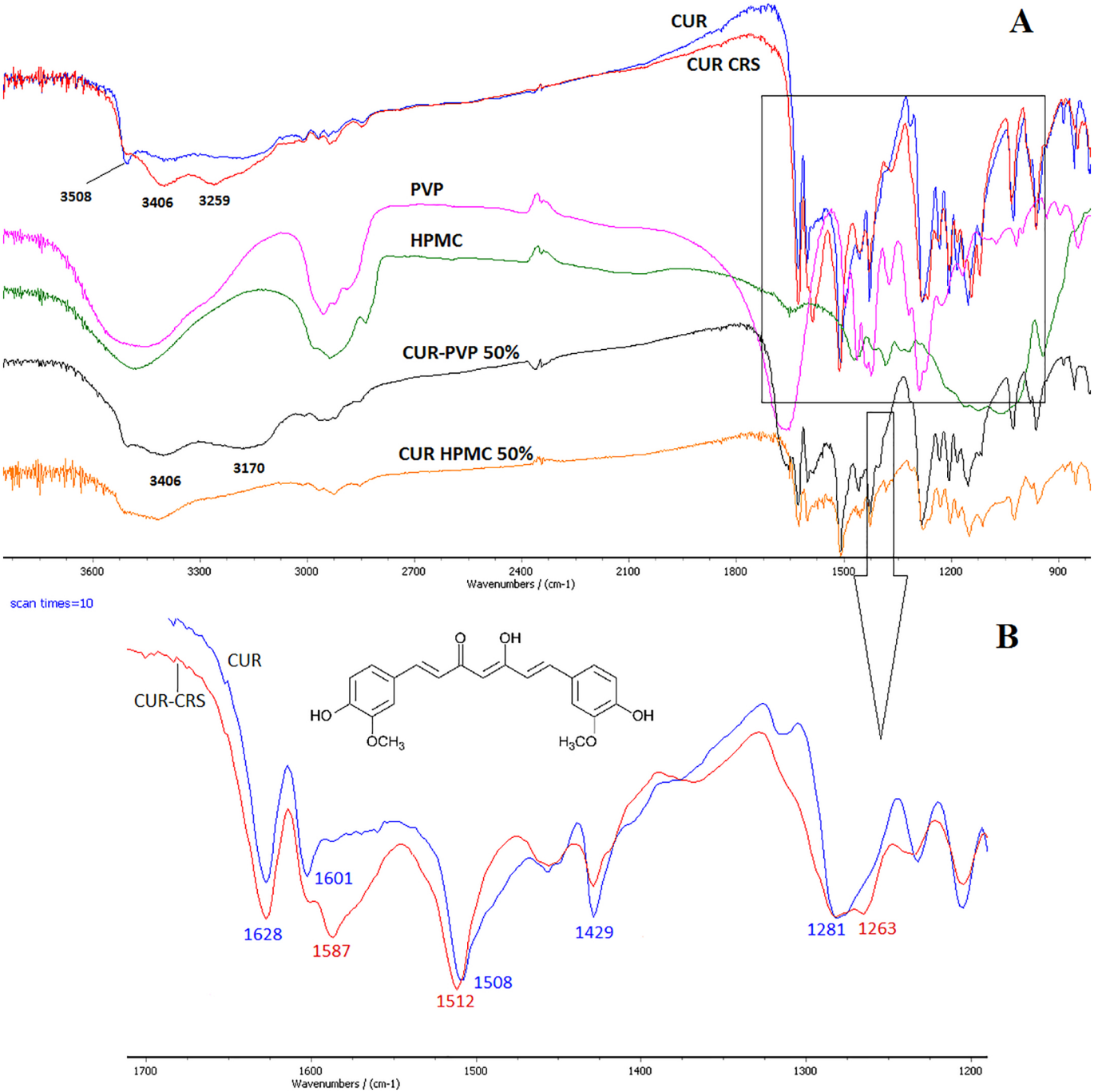
A
CUR
CUR CRS
3508
3406
3259
PVP
HPMC
CUR-PVP 50%
3406
3170
CUR HPMC 50%
3600
3300
3000
2700
2400
2100
1800
1500
1200
900
Wavenumbers / (cm-1)
scan times=10
B
CUR
CUR-CRS
O
OH
HO
OCH3
H3CO
OH
1628
1601
1587
1512
1508
1429
1281
1263
1700
1600
1500
1400
1300
1200
Wavenumbers / (cm-1)

Figure 6

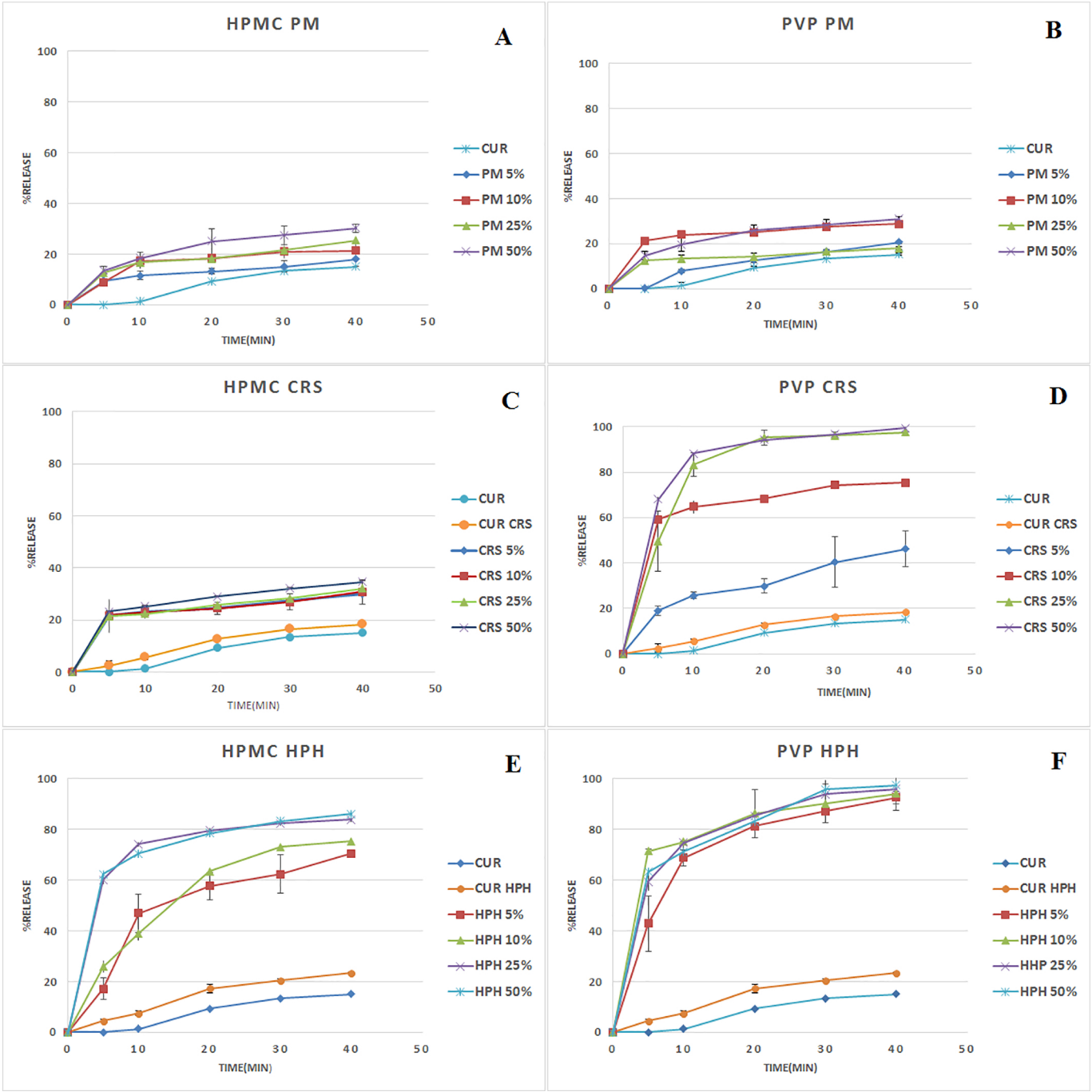
HPMC PM
A
%RELEASE
TIME(MIN)
CUR
PM 5%
PM 10%
PM 25%
PM 50%
PVP PM
B
%RELEASE
TIME(MIN)
CUR
PM 5%
PM 10%
PM 25%
PM 50%
HPMC CRS
C
%RELEASE
TIME(MIN)
CUR
CUR CRS
CRS 5%
CRS 10%
CRS 25%
CRS 50%
PVP CRS
D
%RELEASE
TIME(MIN)
CUR
CUR CRS
CRS 5%
CRS 10%
CRS 25%
CRS 50%
HPMC HPH
E
%RELEASE
TIME(MIN)
CUR
CUR HPH
HPH 5%
HPH 10%
HPH 25%
HPH 50%
PVP HPH
F
%RELEASE
TIME(MIN)
CUR
CUR HPH
HPH 5%
HPH 10%
HHP 25%
HPH 50%

Figure 7

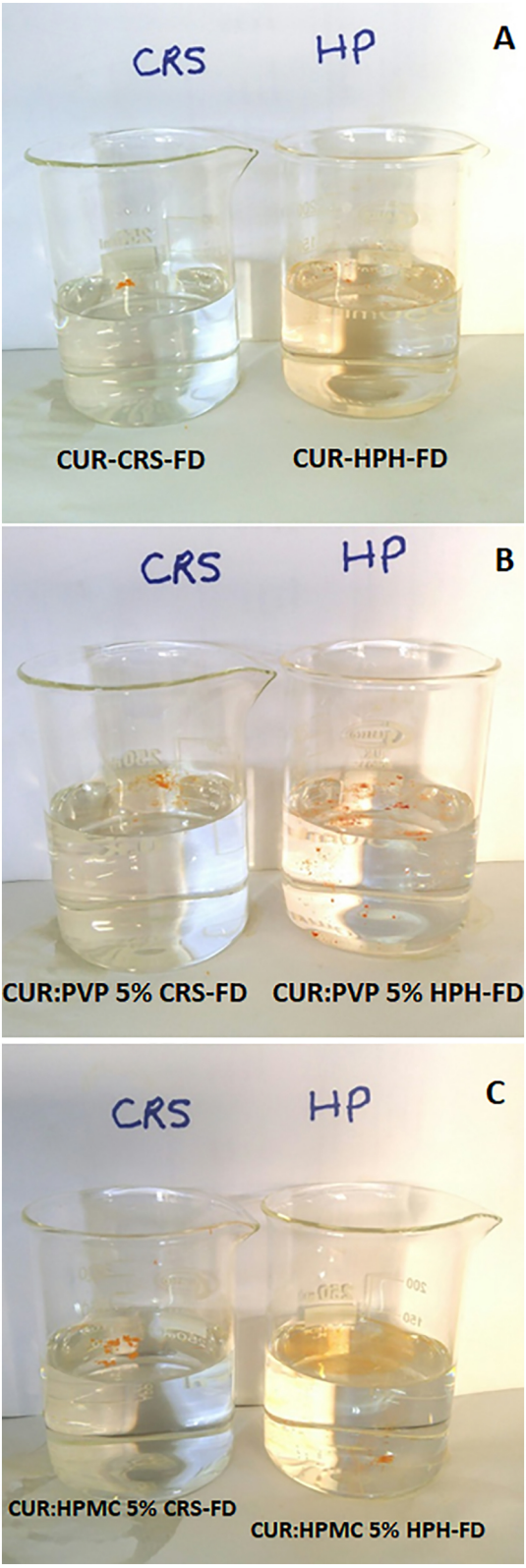
CRS
HP
A
CUR-CRS-FD
CUR-HPH-FD
CRS
HP
B
CUR:PVP 5% CRS-FD
CUR:PVP 5% HPH-FD
CRS
HP
C
CUR:HPMC 5% CRS-FD
CUR:HPMC 5% HPH-FD

Figure 8